Turkish Journal of Electrical Engineering & Computer Sciences

http://journals.tubitak.gov.tr/elektrik/

Research Article

Turk J Elec Eng & Comp Sci
(2016) 24: 2053 – 2070

doi:10.3906/elk-1401-261

Automatic detection of coronary artery disease using registration of ultrasound images of the heart (echocardiography)

Seyed Mohammad ALAVI[1], **Pedram MASAELI**[2,*]
[1]Faculty of Electrical Engineering, Imam Hossein University, Tehran, Iran
[2]Department of Electrical Engineering, Imam Hossein University, Tehran, Iran

Received: 28.01.2014 • **Accepted/Published Online:** 01.07.2014 • **Final Version:** 15.04.2016

Abstract: Coronary artery diseases cause more than half of all deaths in the world. Obviously, early identification is an important way to control coronary artery disease that is diagnosed by measurement and scoring the general and regional movement of the left ventricle of heart (normal, hypokinetic, and akinetic). The most common method of imaging the heart using ultrasound is called echocardiography. Using this method accurate views of the heart walls, valves, and beginning of main arteries can be obtained. Due to the difficulty of the interpretation of these images, the length of time required, and errors in manual methods, an automated analysis method is required. In line with this goal, in this paper we have calculated the displacement field in a cycle of heart motion from two-dimensional echocardiography images. To do this, a frame is usually chosen as the reference frame and then all images in a cycle are mapped to it with a mathematical equation. The main idea is to find a semilocal spatiotemporal parametric model for deformation created in a cardiac cycle with nonrigid registration using B-spline functions as an optimization problem that effectively corrects differences due to movements by minimizing the difference between current frame and a reference frame. Motion estimation accuracy is measured using sum of squares differences. We use a gradient-descent algorithm and multiresolution method to acquire the coefficients in the motion model. The accuracy of the proposed method is assessed using a synthesis sequence of cardiac cycles produced with the simulation software Field II. This algorithm can be applied for the clinical analysis of the regional left ventricle and then movement parameters and threshold values for the scoring of each section can be extracted. The algorithm represents the significant difference between a part of a normal heart and an unhealthy heart and shows the potential of the clinical applications of the proposed method.

Key words: Echocardiography, Field II, B-spline functions, registration, spatiotemporal model, coronary artery disease

1. Introduction

Ultrasound imaging of the heart is called echocardiography. Echocardiography is the most common method for imaging of the left ventricle. Thanks to the low cost, high temporal resolution, noninvasiveness, and short imaging time, it is preferred over other imaging methods such as cardiac magnetic resonance, positron emission tomography, and computed tomography [1]. In this method, one can make two-dimensional images from different sections of the heart using ultrasound and obtain an accurate view of the walls of the heart valves and the beginning of the large arteries [1].

In the usual method, the doctor analyzes the echocardiographic images and follows features that indicate the presence or absence of heart disease. Due to the length of time for a training course needed for interpretation

*Correspondence: pedrammasaeli@yahoo.com

of the images, longevity, and error in manual methods, an automatic analysis is needed. These methods are scientific, accurate, rapid, and independent of subjective opinions [2].

The estimation of cardiac motion is a great solution to quantify the elasticity and force of contraction of heart muscles. Certain areas that have unusual movements indicate that there is ischemia caused by inadequate tissue microcirculation [3,4].

Several methods have been proposed for the analysis of two-dimensional echocardiographic sequences. The most famous is segmenting the heart borders using mechanical and deformable models [3,4]. In these methods, with geometric and mechanical models, using active boundaries or surfaces, a displacement field is extracted and cardiac motion is analyzed. These methods try to overcome complexities of echocardiographic data using a statistical model of motion and the shape of the heart muscle [3,4]. However, these methods estimate the motion of the heart considering the myocardial borders only. As a result, when the motion is parallel to the boundary, we estimate a wrong movement. Another problem with these methods is that boundaries are not always clear in echocardiographic data [4].

Another solution is to use an optical flow method to calculate the local motion of the heart [4]. The main idea of this method is based on the assumption that the light intensity over time and in different regions of the consecutive image frames remains constant. Considering this assumption, the movement area of an image is specified by the constant light pixels and represented by vectors. Nevertheless, this assumption is not always true [5]. In other words, it is possible that illumination of different regions is changed in sequential frames and ignoring this fact will cause an error. This restriction causes the heart movement, especially rotation, not to be detected properly. These movements cause an area of the heart to appear or disappear in the new frame that is not present in the previous frame, leading to changes in the illumination of that area [5].

The third method is cardiac motion tracking and muscle deformation using speckle tracking and elastography techniques. These methods are based on radiofrequency (RF) signal processing to obtain displacement using phase correlation techniques [4].

Tension measurement is another good way to identify areas of heart contraction. Tension measurement to calculate regional myocardial ability deformation is shown by Doppler technique [6,7]. However, estimation of this parameter from Doppler images is limited by angular dependence that does not produce all components of the strain. Using magnetic resonance imaging (MRI), all its components (radial, longitudinal, and peripheral) are created simultaneously for all parts of the heart. However, this method is expensive and it takes a long time to collect the data [6,7].

In this paper, we propose using a nonrigid parametric motion estimation algorithm for echocardiographic image tracking. Our approach is general. It considers all frames with a sequence together and tries to find the best general spatiotemporal motion field. The deformation field is displayed using a parametric model based on B-spline basis functions. The algorithm does not require the segmentation of the heart, which is difficult in ultrasound images [4,8]. The spatiotemporal parametric model with a multiresolution optimization strategy is a good method for tracking the motion of the heart. The multiresolution optimization strategy increases speed and the signal to noise ratio [9–11].

This paper consists of the following parts. In Section 2, we explain the procedure with its details. In Section 3, we evaluate the algorithm for simulated sequences of realistic cardiac motion model. In Section 4, we show results of a clinical application in which regional cardiac analysis of the left ventricle was performed in a group of healthy subjects and patients.

2. Methods

2.1. Problem definition

The sequence of echocardiographic images is called f(t,x) so that t = 0,1,. . . ,T-1, x = (x_1,x_2)ε I where f(t,x) is the intensity at time t and location x. Here, I is the coordinates of the region of interest of the image and T is the number of frames per cycle. Our goal is to find a displacement field in the whole sequence of images. To achieve this aim, a deformation function named g(t, x) is defined, which indicates the location of a point at time t that was at location x at time t = 0. In other words, the first frame is used as a spatial reference. In clinical applications typically an end-diastolic frame is chosen as the reference frame [4,12].

2.2. Deformation function

In our algorithm, fr and ft are N-dimensional discrete reference and test images. The test image is a geometrically deformed version of the reference image, and vice versa. This theorem means that points with the same x coordinate of the reference image fr (x) and the warped test image of $f_w(x) = f_t(g(x))$ should be considered together under the mapping. Here g (x) is the deformation function that should be identified. N is the number of image pixels, and $f_t^c(g(i))$ is the continuous version of the warped test image [13].

2.3. Image interpolation

As introduced, each point in the test image corresponds to a point in the reference image under the mapping function. Because the integral coordinates of the first image may be mapped to the nonintegral coordinates under the mathematical function, a number of integral coordinates and many nonintegral ones will be obtained. Consequently, it is necessary to use an interpolation to create the integral coordinates. We interpolate the image using B-spline basis functions [13].

$$f_t^c(x) = \sum b_i \beta_n(x) \tag{1}$$

Here, β_n is a tensor product of B-splines of degree n such that:

$$X = (x_1, x_2 \ldots x_N),$$

$$\beta_n(x) = \prod_{k=1}^{N} \beta_n(x_k).$$

In all experiments, n = 3 is selected.

2.4. Similarity criteria

Our registration method attempts a minimum value for a criterion, E, which is defined as the mean value obtained from the entire sequence of an image similarity criterion, E_t [4,10,11].

$$E = \frac{1}{T} \sum_{t=0}^{T-1} E_t \tag{2}$$

$$E_t = \frac{1}{N_I} \sum_{i \in I} (f(t, g(t,i) - f(0,i))^2 \tag{3}$$

Here, T is the total number of images in a sequence, I is proportional to the region of interest, and N_I is the number of pixels. Image criterion E_t is the mean square of the differences with the registered image to the reference image at time t = 0. This criterion is selected thanks to its simplicity, rapid computation time, and smoothness of result [4].

In this way, the end-diastolic frame is selected as the reference frame because this frame is easily determined in cardiac image sequences using the R-wave in electrocardiographic signals [4].

2.5. Spatiotemporal model

The deformability function, g(t, x), is expressed by a linear model with parameters $d_{j,l}$, which is separable in time and space.

$$g(t,x) = x + \sum\nolimits_{l \in L} \sum\nolimits_{j \in J} d_{j,l} \varphi_j(x) \psi_L(t) \tag{4}$$

Here, a rectangular grid with specified dimensions (number of control points) is placed on a variable image so as to follow the reference image and minimize error during the registration process [4,14]. In our experiments, the image is determined by 23 longitudinal points and 23 transversal points. That means a total of 529 control points are selected on the image. Parametric functions $\varphi_j(x)$ are defined as the basic functions in the spatial direction and are responsible for spatial smoothness, and $\psi_L(t)$ are time-critical functions that create the temporal relationship of the deformation [14]. Spline functions are a good choice for spatial basic functions $\varphi_j(x)$. These functions are also used for temporal basic functions $\psi_L(t)$, thanks to ease of computation, good approximation, and their smoothness [15]. Other choices are polynomial functions, harmonic functions, radial basis functions, and wavelets. The reason for not using polynomial functions is that there is no fast algorithm to compute them. In radial basis functions, although algorithms to calculate them are not complex, the total number of required processing steps is not negligible. The harmonic functions are forgone due to their weakness in extension of the linear functions. In a comparison between splines and wavelets, a spline is of higher efficiency and its interpolation operation is easier [16].

$$\varphi_j(x) = \beta^n \left({}^{x_1}/_{h} - j_1 \right) \beta^m \left({}^{x_1}/_{h} - j_2 \right) \tag{5}$$

$$j = (j_1, j_2)$$

$$\psi_L(t) = \beta^n \left({}^{t}/_{s} - l \right) \tag{6}$$

Basic functions $\varphi_j(x)$ are located on a uniform rectangular spatial grid and $\psi_L(t)$ can be placed on a regular interval basis. Scaling parameters h and s control answer smoothness and flexibility in problem solving. n and m are used as degrees of splines and typically B-spline functions of degree 2 for $\varphi_j(x)$ and B-splines functions of degree 3 for $\psi_L(t)$ are selected with s = 5 and h = 32 [4].

2.6. Optimization method and multiresolution

The answer to the registration problem is to find the deformation field in such a way that criterion E is minimized. This answer is obtained using a multidimensional optimization algorithm that is applied on the

coefficients d (j, l). If we derive from E a function with respect to the coefficients, then [17]:

$$\frac{\partial E}{\partial d_{j,l,m}}=\frac{1}{N_I T}\sum_{k=0}^{T-1}\sum_{i\in I}2(f\left(t,g\left(k,i\right)\right)-f\left(0,i\right)\frac{\partial f\left(t,x\right)}{\partial x_m}-\frac{\partial g_m\left(k,i\right)}{\partial d_{j,l,m}}. \tag{7}$$

With g (t, x) and f (t, x) of the above equation, we have:

$$\frac{\partial g_m\left(t,x\right)}{\partial d_{j,l,m}}=\beta^n\left({}^t/_s-l\right)\left(\beta^n\left({}^{x_1}/_h-j_1\right).\beta^n\left({}^{x_2}/_h-j_2\right)\right) \tag{8}$$

$$\frac{\partial f(t,x)}{\partial x_m}=\sum_{i\in Z^2}b_{i,t}\beta^n\left(x_m\right)\beta^n\left(x_\mu-i_\mu\right) \tag{9}$$

The gradient-descent method is used to obtain the coefficients. The multiresolution method can also be used to model motion. Thus, first, a deformation function g(t, x) with a few parameters d(j, l) is defined. Then the number of parameters for the best model is obtained. After converging at a certain level, the results can be used as an initial estimation to the appropriate level [18]. In experiments the number of levels is equal to 3 using a trial-and-error method.

3. Experiments with simulated data

Because there is no actual movement of the heart, the only way to accurately test and evaluate the proposed algorithm is using simulated data that are close to reality [19]. In this simulation, we use Malchenko's work. Heart surface motions are expressed with a spline function and spherical coefficients in time and the heart is displayed with mesh [19]. The purpose of this simulation is to extract RF signals from cardiac echocardiography so that it can be applied in Field II [19].

In this way the heart wall is simulated with nested layers whose number can be adjusted at one's discretion. Points located on the wall correspond to scatterers and this is useful in taking pictures of echocardiography. To achieve a more realistic case from the regular points located on the surface, random points are selected. We know that the left ventricular wall is thicker; consequently, to achieve the above-mentioned purpose, such a model is created whose number of scatterers is greater in the left ventricle.

In this model, contraction time is 0.77 s and heart rate is 78 beats per minute. After simulation of wall motion, its movement will be shown in 31 frames in the film. The number of images can be variable. A greater number corresponds to a greater sampling rate. Figure 1 shows a frame of the heart wall with two layers.

In this section, to evaluate the performance of the algorithm, we will examine simulated heart images in Field II software in two different ways: first with all frames on the reference frame and second with the later frame on the earlier.

3.1. Registration of all frames on reference frame

In this section, all frames in sequence will be mapped on the reference frame directly. Figure 2 shows the images of two selected frames registered on the reference frame and mesh changes during the process.

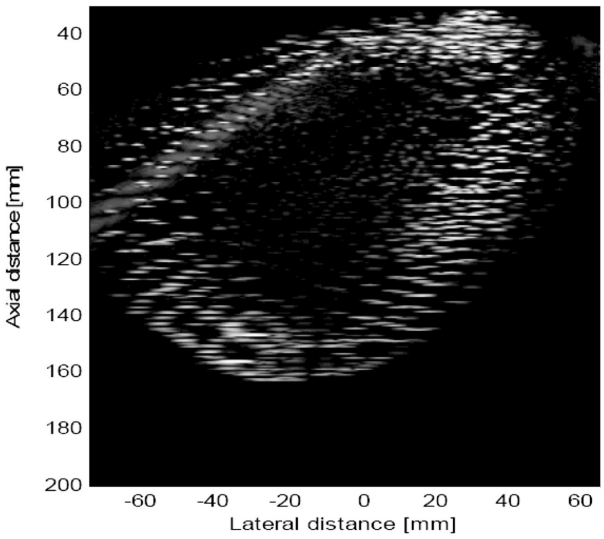

Figure 1. Simulation of the heart wall with Field II software.

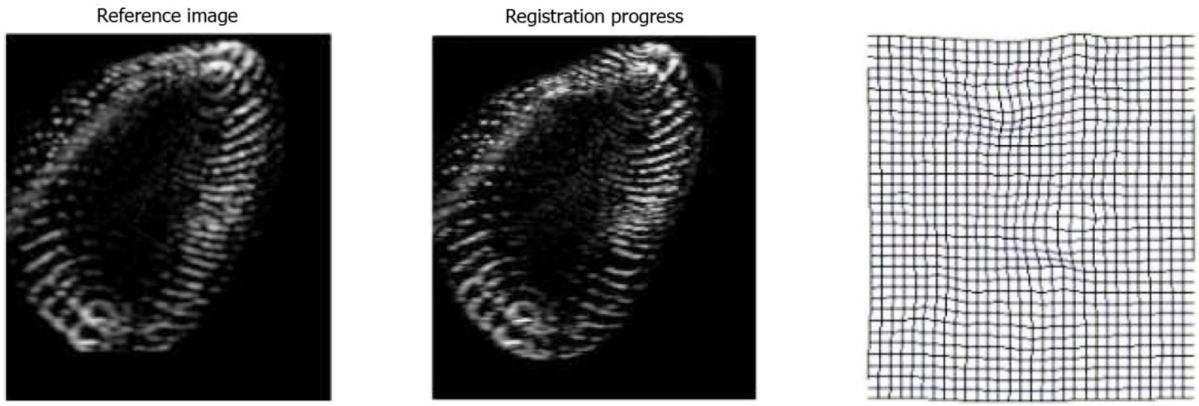

Figure 2. Registration of all frames on reference frame for simulated data and mesh changes during the process.

In this method, after registration of images, the mean of the sum of the square differences in the optimization algorithm during one cycle is equal to 326.36.

3.2. Registration of next frame on previous frame

In this method, each frame in sequence starting from the reference frame is mapped directly to the previous frame. Figure 3 shows the images of two selected frames registered on the previous frames starting from the reference frame and mesh changes during the process.

Here, the mean of the sum of the square differences in the optimization algorithm during one cycle is equal to 280.21.

In the simulated data, it can be seen that the error in all sequences in the registration method of next frame on previous frame is less than in registration of all frames on the reference frame.

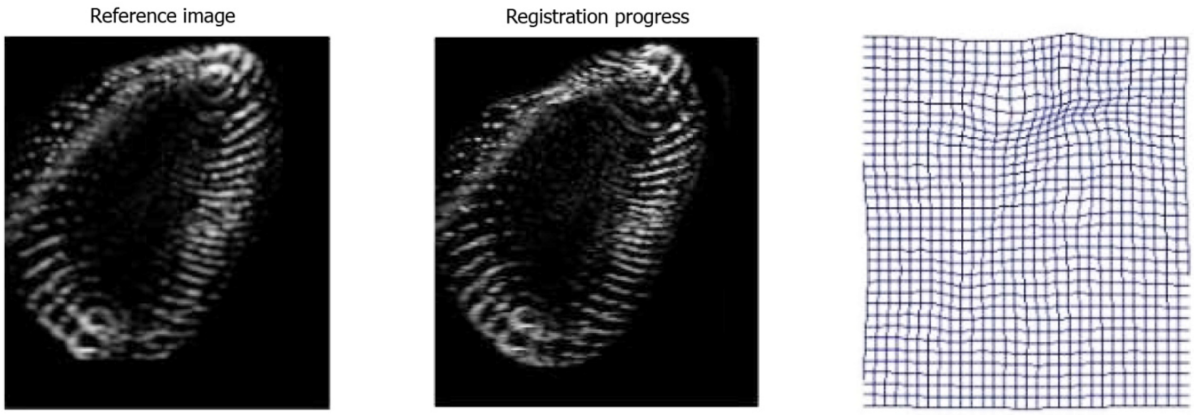

Figure 3. Registration of next frame on previous frame for simulated data and mesh changes during the process.

4. Clinical applications of algorithm and results

In this section, experiments have been conducted to evaluate the efficiency of this algorithm. From echocardiographic sequences, a frame is extracted as the reference frame (usually at end of diastole), and the registration process is done by two methods (registration of all frames on the reference frame and registration of the next frame on the previous frame) and compared. In both methods, the process is performed on all frames of sequences continuously, so it is called group registration. Motion estimation accuracy is measured by using the sum of the square differences criterion.

First, we consider an echocardiographic file as the video. By converter software, we recognize the file as a sequence of frames. Therefore, a cardiac cycle is shown as a number of consecutive frames that is proper for our work. We usually consider the end-diastolic frame corresponding to the peak R on the electrocardiography signal as a reference frame, as shown in Figure 4. As a result, a cardiac cycle is the distance from R to R, and the number of frames in this cycle will vary according to the sampling rate and heart rate. Thus, the aim is to register all the frames on the reference frame that is used by the algorithm.

Then it is necessary to separate the margins of the image and the image of the heart cavity remains. Consequently, we use a cut command in our algorithm for all frames of a cycle. As a result, the reference frame will be as shown in Figure 5.

Both registration methods are then implemented in this frame and the results are compared. For testing, we need to initialize a set of parameters at the beginning. It was expressed that the registration process requires a number of control points. A mesh that is placed on the variable image consists of 23 markers in the longitudinal direction and 23 markers along the transverse. As a result, a total of $529 = 23\ times\ 23$ control points are used for the registration process. Therefore, the whole cycle is registered on the reference frame by 529 control points. It means that the spatial status of 529 control points is determined in all frames. Because the size of images equals $301\ times\ 261$ pixels, a control point is placed at approximately every 11 pixels in the longitudinal direction and every 13 pixels in the transverse direction. These values are obtained using the method of trial and error and given the size of the left ventricle the number of control points in the registration process is reasonably acceptable. As mentioned, the similarity criterion is the sum of the square differences.

In this section, the two procedures above are tested on five sequences of different people. (x), (y), and (z) have a healthy heart and (r) and (t) have an unhealthy heart.

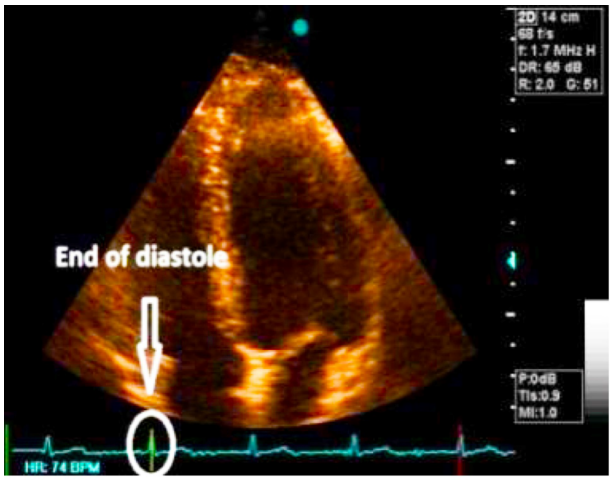

Figure 4. End diastolic frame.

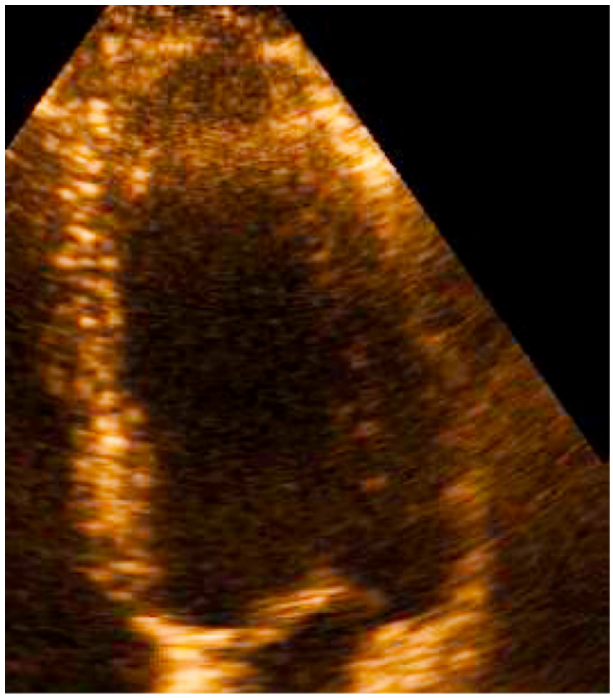

Figure 5. Cut picture of reference frame.

The means of the sum of the square differences during a cardiac cycle in both methods are summarized in Table 1.

Table 1. The mean of sum of the square differences in both methods in echocardiographic sequences of 5 people.

Next frame on previous frame	All frames on first frame	Data
251.2	286.8	(x)
176.6	192.3	(y)
244.4	256.6	z))
161.1	175.6	(r)
234.8	262.5	(t)

As we can see in Table 1, in both methods, the error of the sum of the square differences is greater in healthy subjects than in patients. Considering that the amount of displacement of the heart in healthy subjects is higher than in patients, different parts of the heart in healthy people will have more spatial variability and the error of the sum of the square differences would be greater during the cardiac cycle. This error for all sequences in the registration of the later frame on the earlier frame method is less than in the registration of all frames on the reference frame method. Changes between two consecutive frames in a cardiac cycle are negligible, and this value is less than the variation between two nonconsecutive frames. Therefore, the results of the algorithm will be consistent with our expectations. In clinical applications we will use the second method (registration of the later frame on the earlier frame) thanks to a lower rate of error.

4.1. Regional analysis of the left ventricle

4.1.1. Data collection

Four-chamber sequences of seven individual cases are investigated in this section. These people will be represented with the letters b, d, m, n, f, g, and s. The end-diastolic frame for every person is extracted as the

reference frame. It is assumed that the probe and the patient cannot move at all (when imaging, breath is held).

According to the standard, the view of the four-chamber left ventricle in the reference frame is divided into 7 areas. As a result, the reference frame is divided into 7 zones (A, AS, MS, BS, AL, ML, and BL) with standard lines. For this purpose, first, we consider the reference frame. On the image, we determine point p1 on the apex and points p2 and p3 on the two sides of the mitral valve and we consider an imaginary line between p2 and p3. From the middle of the line, we draw another line to p1. We divide the line into three parts and draw two parallel lines from the division places. In addition, from the second point, we draw two lines at a 60^{circ} angle. It can be seen from these divisions that seven areas are created, as shown in Figure 6.

Seven sections are named as shown in Figure 7.

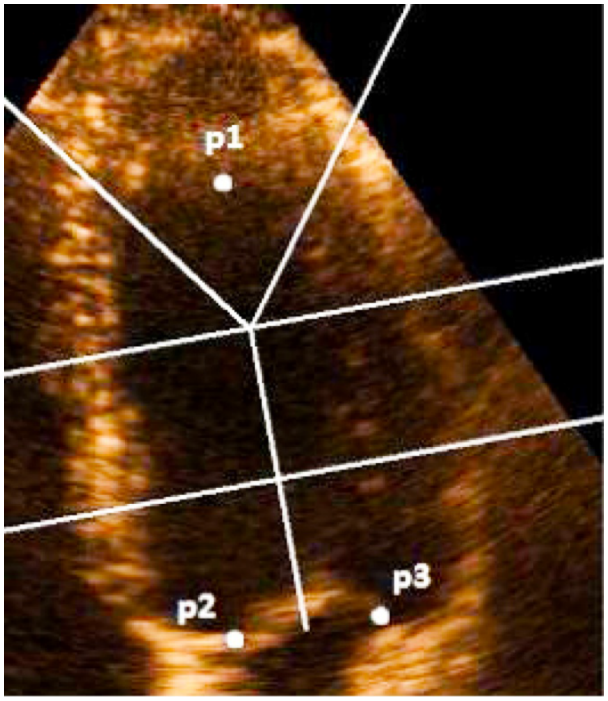

Figure 6. Division of reference frame into seven areas.

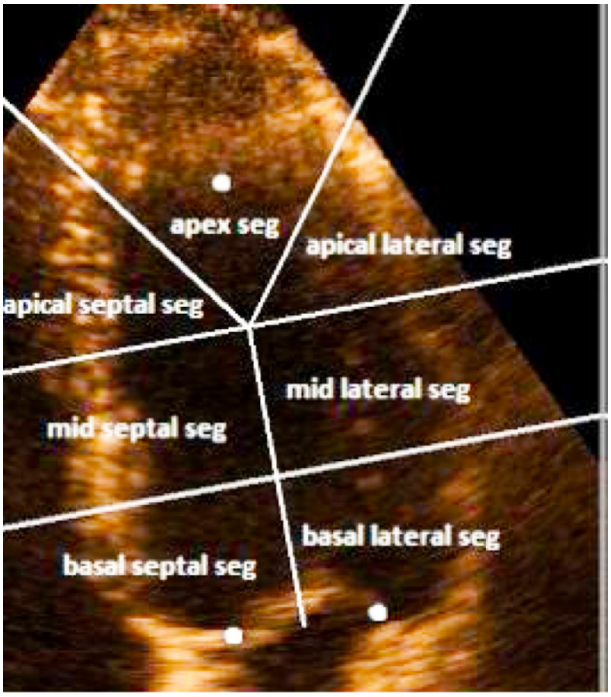

Figure 7. Division of reference frame into seven areas and name sections.

This operation is performed in the reference frame for all 7 people.

According to the American Heart Association standard, the left ventricle was divided into 17 sections that can be specified from 1 to 17. In the four-chamber view of the left ventricle, some of these sections will be visible, whose standard numbers are tabulated respectively in Table 2.

Each selected point of the reference frames is located in one of these 7 zones. As mentioned in the previous section, we use a mesh of 529 control points in the registration process. It is necessary to investigate the status of each selected point of reference frame.

The idea used in this paper is that each of these control points during the registration process of the entire cycle follows a specific path and so has a unique transfer function. Previously, the status of the 529 control points was determined by the registration algorithm. As a result, a control point is assigned to each arbitrary point. Using the fact that each control point has special changes within the frames of the heart,

we select random points on the image. To do this, displacement of each arbitrary point is calculated from all control points. The control point that is closest is assigned to the arbitrary point. Then the path of motion of all points is characterized in the cardiac cycle. For the classification of the selected pixels, we use the minimum distance rule to the control points. Therefore, having any selected pixel P, we can calculate its distance from all 529 control points and derive the lowest value of them. If we assume that the minimum distance is from the control point C_i, this means that pixel P is closer to the control point C_i and its changes are similar to C_i during all frames. Pixel p follows the transfer function of control point C_i. Thus, we will have a transfer function for each chosen pixel of an image. With respect to any chosen point in each of the seven regions of the ventricular wall, with correspondence between this point and its control point, we can draw its motion path. We see the results of four zones of sequences for d and n in the following figures (Figures 8–15). In all figures, the end-diastolic reference frame is marked with number one and point number two displays the location of those points in the second frame. These points will help to recognize the direction of the intended point during the cycle in images.

Table 2. Areas of four chambers view and their standard numbers.

Standard number	Area
17	Apex seg (A)
14	Apical septal seg (AS)
8, 9	Midseptal seg (MS)
2, 3	Basal septal seg (BS)
16	Apical lateral seg (AL)
11, 12	Midlateral seg (ML)
5, 6	Basal lateral seg (BL)

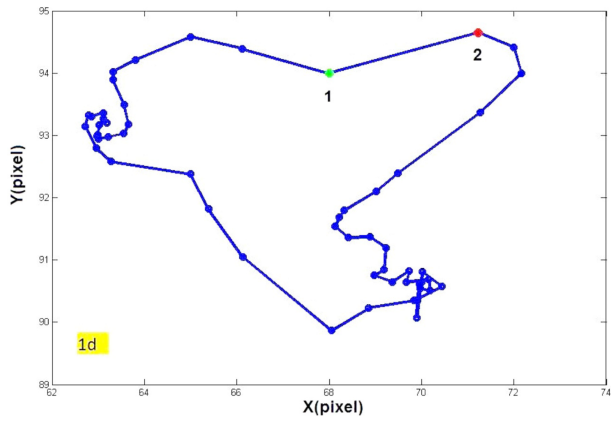

Figure 8. Tracking of chosen point in zone A in cardiac cycle of healthy heart d.

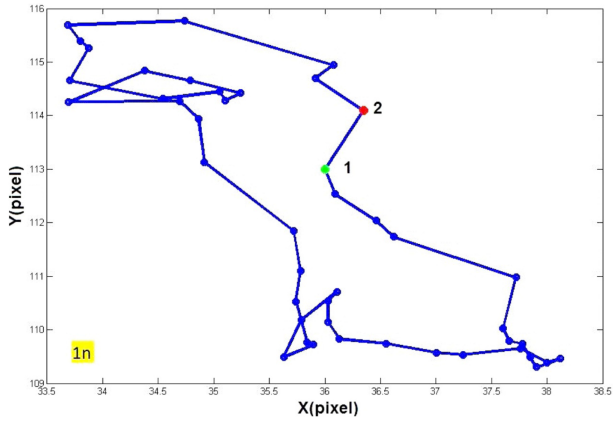

Figure 9. Tracking of chosen point in zone A in cardiac cycle of patient heart n.

4.1.2. The extracted parameters

Our assessment of the cardiac function is done using the maximum displacement of points in the images. In each image, if we show the minimum value of the longitudinal coordinates with X1 and the maximum value of the longitudinal coordinates with X2, XDis is defined as the distance between the two points as follows:

$$XDis = X_2 - X_1. \tag{10}$$

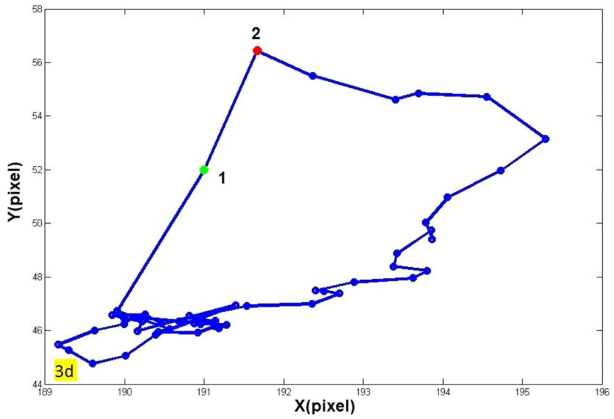

Figure 10. Tracking of chosen point in zone MS in cardiac cycle of healthy heart d.

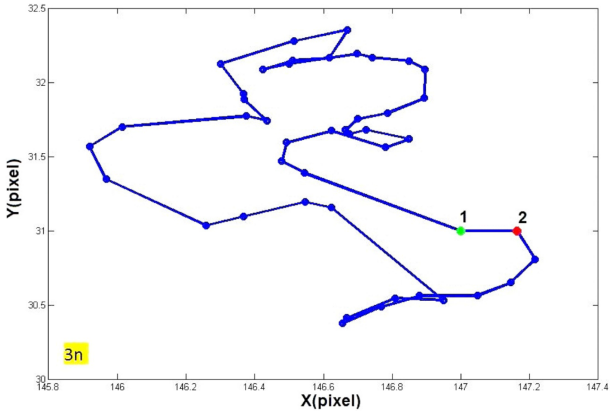

Figure 11. Tracking of chosen point in zone MS in cardiac cycle of patient heart n.

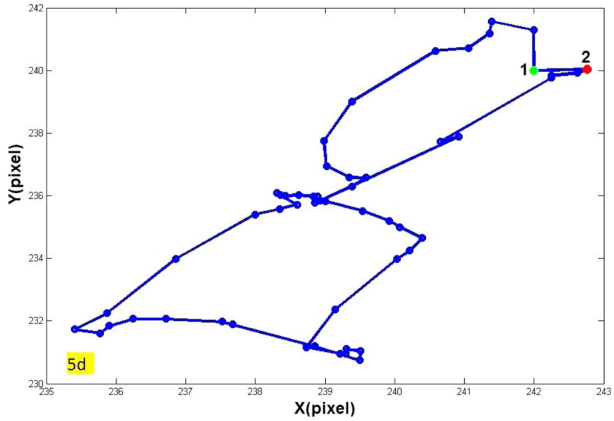

Figure 12. Tracking of chosen point in zone BL in cardiac cycle of healthy heart d.

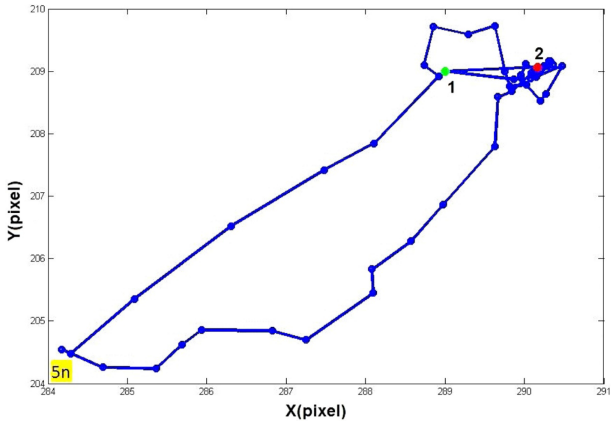

Figure 13. Tracking of chosen point in zone BL in cardiac cycle of patient heart n.

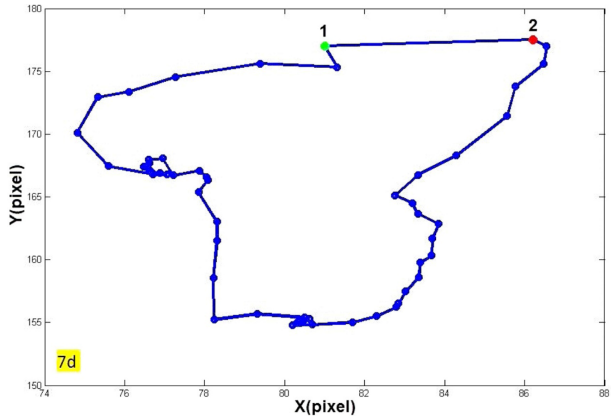

Figure 14. Tracking of chosen point in zone AL in cardiac cycle of healthy heart d.

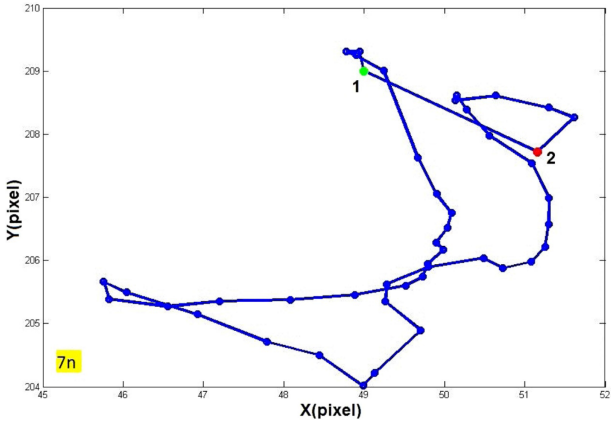

Figure 15. Tracking of chosen point in zone AL in cardiac cycle of patient heart n.

Similarly, if we show the minimum value of the transverse coordinates with Y1 and the maximum value of the transverse coordinates with Y2, YDis is defined as the distance between the two points as follows:

$$Ydis = Y_2 - Y_1. \tag{11}$$

If we show the maximum displacement of any point with Dis, using the Pythagoras equation, we have:

$$Dis = ((XDis)^2 + (YDis)^2)^{1/2}. \tag{12}$$

The displacement parameter will be a criterion to score each of the seven regions of the heart for these people. Heart wall motion is divided into three categories, normal, hypokinetic, and akinetic, based on the displacement. If we plot the measured displacement of these seven people in each part of the heart in separate diagrams, according to the arrangement of these points and comparison of these results with a specialist opinion, we can create three regions (normal, hypokinetic, and akinetic) by placing two threshold values for each part of the heart. With the proper threshold for each of the seven regions, we can attribute one of the three categories to any person. The DIS parameter was defined in accordance with the motion path, which can be obtained about all points. This parameter is a criterion for the classification of each part of the heart. The motion is different in various parts of the heart. For this reason, different thresholds can be defined. As a result, by selecting an arbitrary point that is certainly in one of the 7 zones, a corresponding control point is specified, the path of its motion is drawn, and its DIS parameter is calculated. Compared to the thresholds of the considered zone, the status of that point (normal, hypokinetic, akinetic) is determined.

In the following figures (Figures 16–19) and tables (Tables 3–6), we see the results for each region of each person. The specialist's opinion is given in the final column of each table after seeing echocardiographic images of people in different parts of the heart.

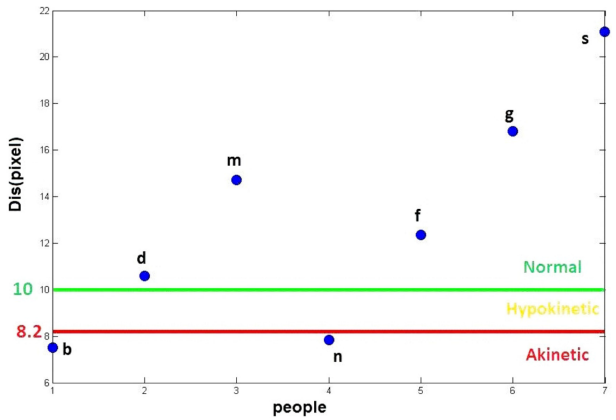

Figure 16. Thresholding in zone A.

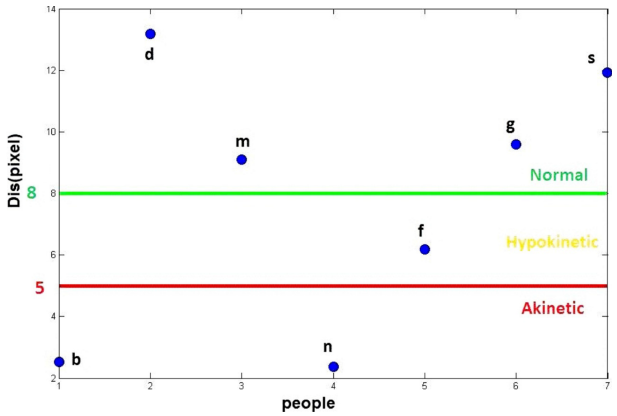

Figure 17. Thresholding in zone MS.

Arrangement of points in the diagram generated through the registration algorithm, compared with the specialist's opinion, can accurately and intuitively be classified into the three categories above. It is enough to determine threshold values for each of the three regions quantitatively. As can be seen in the figures (Figures 16–19), for zone A, two threshold values of 10 and 8.2 are considered for three categories: normal, hypokinetic, and akinetic. Because of the amount of displacement of f with 12.343 pixels, which is higher than both threshold values, its situation is normal in this area. However, due to the displacement of n with 7.837 pixels, which is lower than both thresholds, its situation is akinetic in this zone. Two threshold values are 5 and 8 in the MS

zone. The amount of displacement of f in this zone is 6.176 pixels and its situation is hypokinetic here, and the amount of displacement of n is 2.367 pixels here and its situation is akinetic.

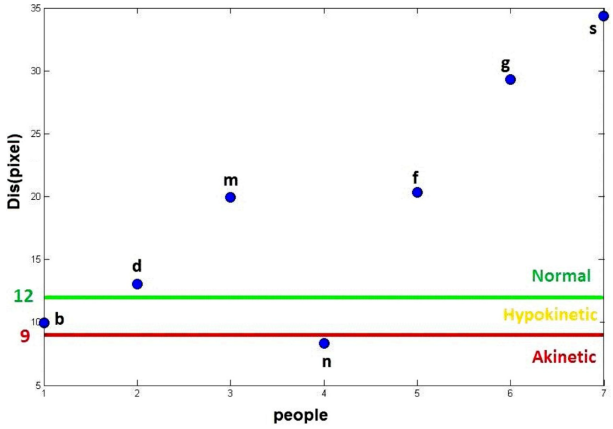

Figure 18. Thresholding in zone BL.

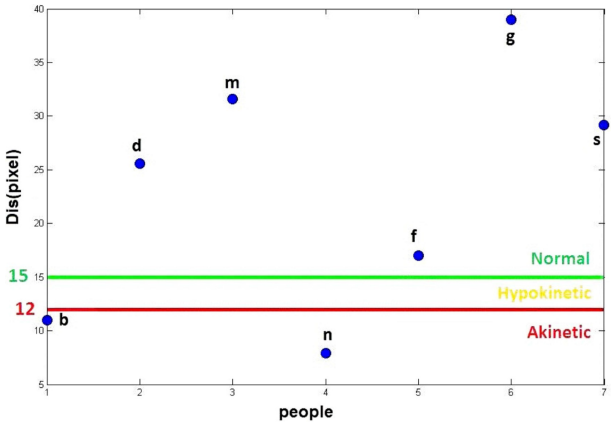

Figure 19. Thresholding in zone AL.

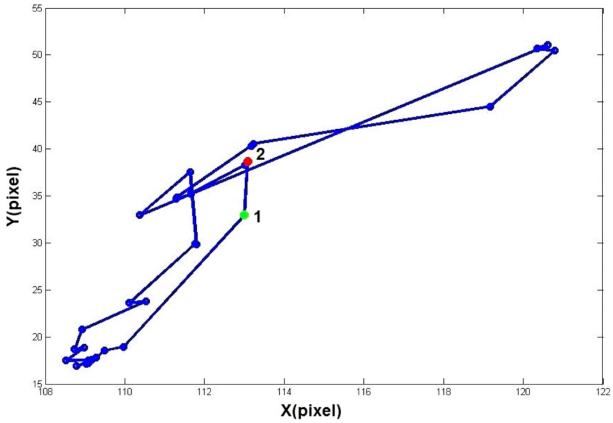

Figure 20. Displacement of first point in simulated data.

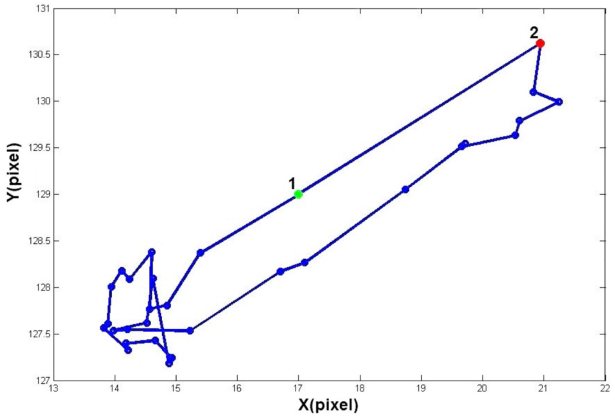

Figure 21. Displacement of third point in simulated data.

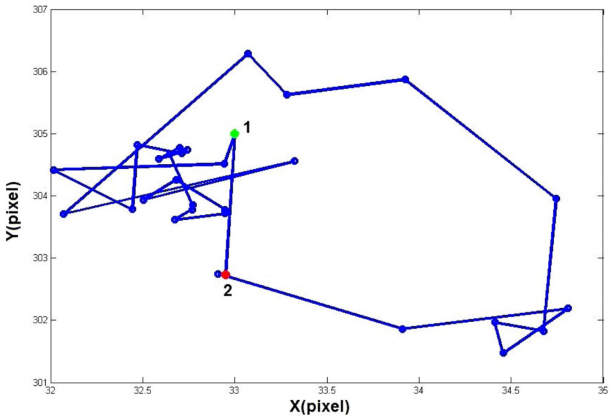

Figure 22. Displacement of fifth point in simulated data.

Table 3. Results of zone A in different people.

Data	Status	X1	X2	XDis	Y1	Y2	YDis	Dis
(b)	Akinetic	28.964	34.733	5.768	92.697	97.493	4.795	7.501
(d)	Normal	62.722	72.156	9.434	89.870	94.651	4.781	10.577
(m)	Normal	51.398	61.662	10.264	84.588	95.117	10.528	14.704
(n)	Akinetic	33.685	38.119	4.433	109.310	115.772	6.462	7.837
(f)	Normal	32.362	40.677	8.315	101.943	111.065	9.122	12.343
(g)	Normal	32.934	46.782	13.847	71.484	81.034	9.549	16.821
(s)	Normal	34.249	45.125	10.876	96.601	114.658	18.056	21.079

Table 4. Results of zone MS in different people

Data	Status	X1	X2	XDis	Y1	Y2	YDis	Dis
(b)	Akinetic	159.297	161.323	2.026	31.526	33.050	1.523	2.535
(d)	Normal	189.166	195.287	6.121	44.766	56.431	11.665	13.173
(m)	Normal	129.519	137.385	7.865	58.599	63.190	4.591	9.107
(n)	Akinetic	145.919	147.215	1.296	30.374	32.353	1.979	2.366
(f)	Hypokinetic	159.431	164.498	5.067	28.654	32.185	3.531	6.176
(g)	Normal	159.054	162.543	3.489	23.098	32.037	8.939	9.596
(s)	Normal	138.498	149.407	10.908	41.711	46.534	4.823	11.927

Table 5. Results of zone BL in different people.

Data	Status	X1	X2	XDis	Y1	Y2	YDis	Dis
(b)	Hypokinetic	236.277	243.986	7.708	155.963	162.270	6.306	9.959
(d)	Normal	235.411	242.763	7.351	230.753	241.557	10.804	13.068
(m)	Normal	281.876	287.620	5.744	226.305	245.392	19.086	19.932
(n)	Akinetic	284.174	290.477	6.303	204.241	209.730	5.488	8.358
(f)	Normal	262.678	278.545	15.867	215.007	227.715	12.707	20.328
(g)	Normal	282.227	297.760	15.532	220.114	244.954	24.840	29.296
(s)	Normal	271.058	297.010	25.951	218.548	241.045	22.497	34.345

Table 6. Results of zone BL in different people.

Data	Status	X1	X2	XDis	Y1	Y2	YDis	Dis
(b)	Akinetic	62.375	69.374	6.999	186.232	194.693	8.461	10.980
(d)	Normal	74.820	86.548	11.728	154.793	177.513	22.720	25.568
(m)	Normal	62.459	88.231	25.771	158.912	177.235	18.323	31.621
(n)	Akinetic	45.751	51.613	5.862	204.018	209.312	5.294	7.898
(f)	Normal	49.444	56.640	7.195	161.931	177.349	15.418	17.015
(g)	Normal	31.403	47.115	15.711	142.424	178.088	35.664	38.971
(s)	Normal	66.974	77.696	10.722	183.043	210.195	27.152	29.192

Due to the different rates of displacement in different parts of the heart, threshold levels in each section are certain. For example, due to more movement of zone A than zone MS, the threshold values in zone A are larger than in zone MS. These numbers are selected according to the method of trial and error experiments with different subjects. In order to determine the threshold values for each sector, we need to increase the number of data and test the echocardiographic sequences of more people (at least 200) by this method. Therefore, clinical application of the algorithm is determined such that the status of each point is characterized with one click.

4.2. Displacement of the simulated data

In this section, we calculate the displacement of 5 random points from simulated sequences after the registration process during 31 heart frames as shown in following figures (Figure 20, Figure 21 and Figure 22):

5. Discussion and conclusion

In this paper, the standard video of echocardiography used was taken by the operator at the hospital in a four-chamber view of the heart. In each one, frequency, imaging rate, and other parameters were set by a device to get more appropriate and better quality images. Thus, diagnosis of heart disease in different parts of the image is also possible by a specialist. However, as noted above, due to the length of time needed and tiresome manual methods, we use the automatic method proposed in the paper to make the diagnosis quantitative, scientific, accurate, and fast.

As a result, noises created in the image due to the inherent noise of ultrasound and device noise are in the range that can be recognized by the specialist and the automatic algorithm. In each of the seven cardiac areas, more than one point is examined to lead to a more acceptable result. If necessary, the method of averaging is used to reduce the effects of noise to contribute to better clinical applications.

The registration problem was mooted to find a semilocal spatiotemporal parametric model for deformation created in a cardiac cycle using B-spline functions. To do this, we chose a frame as a reference frame, and then mapped all the frames in a cycle to that frame using a mathematical equation and, using it, estimated the displacement field of cardiac motion in a cycle.

In this model, the main idea was to find a semilocal spatiotemporal parametric model for deformation created in a cardiac cycle with nonrigid registration using B-spline functions as an optimization problem that effectively corrected differences due to movements by minimizing the difference between the current frame and a reference frame. We used a gradient-descent algorithm and multiresolution method to acquire the coefficients in the motion model.

The proposed algorithm is an automatic method in which the motion situation of each point (normal, hypokinetic, and akinetic) will be determined by clicking on that point on the heart wall. Recent studies on this subject have been conducted with different methods for the analysis of two-dimensional echocardiographic sequences. The most famous is segmenting the heart borders using mechanical and deformable models. In these methods, with geometric and mechanical models, using active boundaries or surfaces, the displacement field is extracted and cardiac motion is analyzed. In fact, these methods try to overcome the complexities of echocardiographic data by using a statistical model of motion and shape of the heart muscle. However, these methods estimate the motion of the heart considering the myocardial borders only. As a result, when the motion is parallel to the boundary, we estimate a wrong movement. Another problem with these methods is that boundaries are not always clear in echocardiographic data. Unlike these methods, which define the exact boundaries of the heart in ultrasound images, which is difficult due to the inherent noise and complicated structure of heart and makes motion estimation incorrect, in our work there is no need for segmentation of the heart wall here. Another method is to use an optical flow method to calculate the local motion of the heart. The main idea of this method is based on the assumption that the light intensity over time and in different regions of the consecutive image frames remains constant. Considering this assumption, the movement area of an image is specified by the constant light pixels and represented by vectors. Nevertheless, this assumption is not always true. In other words, it is possible that illumination of different regions is changed in sequential frames and ignoring this will cause an error. This restriction causes the heart movement, and especially rotation, not to be detected properly. These movements cause an area of the heart to appear or disappear in the new frame

that is not present in the previous frame, leading to changes in the illumination of that area. Unlike optical flow methods, we consider illumination change in different regions of the image in sequential frames by which movements are properly identified when the heart beats. The third method is cardiac motion tracking and muscle deformation using speckle tracking and elastography techniques. These methods are based on RF signal processing to obtain displacement using phase correlation techniques. Tension measurement is another good way to identify areas of heart contraction. Tension measurement to calculate regional myocardial ability deformation is shown by Doppler technique. However, estimation of this parameter from Doppler images is limited by angular dependence that does not produce all components of the strain. Using MRI, all its components (radial, longitudinal, and peripheral) are created simultaneously for all parts of the heart. However, this method is expensive and it takes a long time to collect the data. Unlike other methods, such as radial functions and wavelet, here we used spline functions to reduce the dependency between the parameters and avoid complex calculations. Also, compared to other imaging techniques such as MRI and computed tomography, we will pay a lower cost. Compared to manual methods we will save time, about 30 s, and we can identify the situation of the entire cardiac cycle and displacements of all points in a group registration. Also, the study was undertaken on two images with single registration, which is time-consuming and is required to be on all frames separately. Using group registration in this algorithm, we understand the condition of the heart cycle simultaneously.

We have conducted experiments to evaluate the algorithm, extracted an end-diastolic frame as a reference frame, and performed the registration process by two methods as the next frame to the previous frame and all frames on the first frame and compared them. Then we examined the algorithm for the simulated model of a real heart in Field II. Here we calculated the displacement of five chosen points of the simulated sequence after registration for 31 cardiac frames. Here, the displacement error is the difference between the calculated displacement by the registration algorithm and the heart model. Displacement error in these points is between 11.44% and 19.73%. The model is approximate and the heart wall is considered by two layers for simplicity of mathematical calculations, and movements of the heart cycle were expressed in spherical coordinates with mesh in 31 frames. Obviously, there is a difference between displacement calculated by the model and the algorithm. As a result, simulated data that are tested by this algorithm are different from the data of a real heart because the inherent complexities of the heart were neglected in this section and an approximate model is presented with two layers. Finally, here the aim is to evaluate the capability of the algorithm used to track a point of a reference image during the simulation and plot the motion path of that point during a cycle (31 frames) and whether that can draw the approximate path of motion of all points in 7 segments with various motion paths of different parts of the heart or not. As a result, the range of error in this section is basically acceptable and permitted.

In the end, for clinical applications using four-chamber images, motion in different parts is investigated and these parts are scored by thresholding and comparing the results of the algorithm with a specialist's opinion. Due to the different displacement of seven parts of the left ventricle, we chose different threshold values for each part to assess the extent of its movement. Also, we traced the motion path of a selected point of the heart wall during a cardiac cycle and showed the results in tables and graphs so that the rate of displacement was evident in each area. However, in real images taken from people, precise tracking is done by setting frequency, imaging rate, and other parameters. Consequently, despite the inherent noise of echocardiographic images and device noise, the quality of the images was good. With access to a reasonable amount of parameter means of the sum of the square differences (range of 200 to 400), we get proper images such that the heart wall is detectable and dividing it into seven regions and the registration process are easily done. As a result, displacement of different parts of the heart is calculated by the parameter DIS. An appropriate threshold for each section shows the

condition of various sectors of heart. This parameter is a criterion to evaluate heart health. Results showed significant differences between normal and patient hearts.

The results showed that this technique could be a way to evaluate the cardiac muscle motion in echocardiographic data. As future research activities, we can propose a method for registration in three-dimensional echocardiographic images.

We can also test other views in different people, such as two-chamber, long-axis, and short-axis views, and achieve more accurate information of the heart vessels with respect to all areas of the heart.

This method investigates the rate of left ventricular wall motion. Similar research can be performed on images of the right ventricle, checking the possible diseases of this cavity.

In the proposed algorithm other parameters such as the environment caused by tracking the chosen point of the heart wall during the cardiac cycle or the area enclosed by the path of that point could be the basis for calculation and the classification of people.

Automation of the process of selecting an appropriate threshold in different parts of the heart can be considered as further research activities. To do this, there is a need for available data from more subjects (at least 200 people) to determine the value of each threshold accurately.

References

[1] Noble JA, Boukerroui D. Ultrasound image segmentation: a survey. IEEE T Med Imaging 2006; 25: 987-1010.

[2] Bosch JG, Mitchell SC, Lelieveldt BF, Nijland F, Sonka M, Reiber JC. Automatic segmentation of echocardiographic sequences by active appearance motion models. IEEE T Med Imaging 2002; 21: 1374-1383.

[3] Carranza N, Cristobal G, Ledesma-Carbayo MJ, Santos A. A new cardiac motion estimation method based on a spatio-temporal frequency approach and Hough transform. Comput Cardiol 2006; 33: 805-808.

[4] Ledesma-Carbayo MJ, Kybic J, Desco M, Santos A, Sühling M, Hunziker P, Unser M. Spatio-temporal nonrigid registration for ultrasound cardiac motion estimation. IEEE T Med Imaging 2005; 24: 1113-1126.

[5] Sühling M, Arigovindan M, Jansen C, Hunziker P, Unser M. Myocardial motion analysis from B-mode echocardiogram. IEEE T Med Imaging 2005; 14: 525-536.

[6] Ledesma-Carbayo MJ, Santos A, Kybic J, Mahia-Casado P, Fernandez G, Malpica N, Perez E. Myocardial strain analysis of echocardiographic sequences using non-rigid registration. Comput Cardiol 2004; 31: 313-316.

[7] Barcaro U, Moroni D, Salvetti O. Automatic computation of left ventricle ejection fraction from dynamic ultrasound imaging. Lect Notes Comput Sc 2008; 18: 351-358.

[8] Zitova B, Flusser J. Image registration methods: a survey. Image Vision Comput 2003; 21: 977-1000.

[9] Makela DT, Clarysse P, Sipila O, Pauna N, Pham Q, Katila T, I. Magnin I. A review of cardiac image registration methods. IEEE T Med Imaging 2002; 21: 1011-1021.

[10] Hill DG, Batchelor PG, Holden M, Hawkes DJ. Medical image registration. Phys Med Biol 2001; 46: 1-45.

[11] Rueckert D, Aljabar P. Nonrigid registration of medical images: theory, methods, and applications. IEEE Signal Proc Mag 2010; 27: 113-119.

[12] Malpica N, Santos A, Zuluaga MA, Ledesma MJ, Perez E, Fernandez MG, Desco M. Tracking of regions of interest in myocardial contrast echocardiography. Ultrasound Med Biol 2004; 30: 303-309.

[13] Kybic J. Fast parametric elastic image registration. IEEE T Image Process 2003; 12: 1427-1442.

[14] Ledesma-Carbayo MJ, Santos A, Kybic J, Mahia-Casado P, Fernandez G, Malpica N, Perez E. Cardiac motion analysis from ultrasound sequences using nonrigid registration: validation against Doppler tissue velocity. Ultrasound Med Biol 2006; 32: 483-490.

[15] Xie Z, Farin GE. Image registration using hierarchical B-splines. IEEE T Vis Comput Gr 2004; 10: 85-94.

[16] Mahia P, Ledesma-Carbayo MJ, Verdugo V, David EP, Santos A, Moreno M, Menendez MD, Fernandez MA. Radial versus longitudinal myocardial deformation from gray-scale echocardiography. Ultrasound Med Biol 2007; 33: 1699-1705.

[17] Rueckert D, Sonoda LI, Hayes C, Hill DG, Leach MO, Hawkes DJ. Nonrigid registration using free-form deformations: application to breast MR images. IEEE T Med Imaging 1999; 18: 712-721.

[18] Odobez JM, Bouthemy P. Robust multiresolution estimation of parametric motion models. J Vis Commun Image R 1995; 6: 348-365.

[19] Jensen JA. Field II: A program for simulating ultrasound systems. Med Biol Eng Comput 1996; 34: 351-353.